HHS Public Access

Author manuscript

Radiother Oncol. Author manuscript; available in PMC 2020 January 01.

Published in final edited form as:

Radiother Oncol. 2019 January ; 130: 46–55. doi:10.1016/j.radonc.2018.08.010.

A Prospective Longitudinal assessment of MRI Signal Intensity Kinetics of Non-Target Muscles in Patients with Advanced Stage Oropharyngeal Cancer in Relationship to Radiotherapy Dose and Post-Treatment Radiation-Associated Dysphagia: Preliminary findings from a Randomized Trial

Joint Head and Neck Radiotherapy-MRI Development Cooperative MeheissenMohamed A. M.1,5MohamedAbdallah S. R. 1,5,6KamalMona1HernandezMike4VolpeStefania1ElhalawaniHesham1BarrowMartha P. 3DingYao1WangJihong2DavuluriRaj3RostomYousri5HegazyNeamat5GunnG.Brandon1LaiStephen Y.3GardenAdam S.1LewinJan S.3RosenthalDavid I.1FrankSteven J.1FullerClifton D. 1HutchesonKatherine A.3

[1]Department of Radiation Oncology, The University of Texas MD Anderson Cancer Center, Houston, TX, USA

[2]Department of Radiation Physics, The University of Texas MD Anderson Cancer Center, Houston, TX, USA

[3]Department of Head and Neck Surgery, The University of Texas MD Anderson Cancer Center, Houston, TX, USA

[4]Department of Biostatistics, The University of Texas MD Anderson Cancer Center, Houston, TX, USA

[5]Department of Clinical Oncology and Nuclear Medicine, Faculty of Medicine, University of Alexandria, Alexandria, Egypt

[6]MD Anderson Cancer Center UTHealth Graduate School of Biomedical Science, Houston, TX, USA.

Abstract

Purpose: To assess quantitative signal intensity (SI) kinetics obtained from serial MRI of swallowing muscles as a potential imaging biomarker of radiation-induced dysphagia in oropharyngeal cancer (OPC) patients receiving radiotherapy (RT).

[*]**Co-corresponding Authors:** -Clifton D. Fuller, MD, PhD, Head and Neck Section, Division of Radiation Oncology, Department of Radiation Oncology, The University of Texas MD Anderson Cancer Center, Box 0097, 1515 Holcombe Blvd., Houston, TX, 77030, Phone: 713-563-2334, Fax: 713-563-2366, cdfuller@mdanderson.org; - Katherine Hutcheson, PhD, Department of Head and Neck Surgery, The University of Texas MD Anderson Cancer Center, 1515 Holcombe Blvd., Houston, TX, 77030, Phone: 713-792-6513, KArnold@mdanderson.org; - Steven J. Frank, M.D., Head and Neck Section, Division of Radiation Oncology, Department of Radiation Oncology, The University of Texas MD Anderson Cancer Center, Box 0097, 1515 Holcombe Blvd., Houston, TX, 77030, Phone: 713-563-2334, Fax: 713-563-2366, sjfrank@mdanderson.org.

Conflict of interest statement: The authors declare no conflicts of interest.

Methods: Patients were enrolled under an IRB approved Phase II/III randomized trial. Patients underwent serial MRIs at pre-, mid-, and post-RT. Normalized T1, T1+ contrast (T1+C), and T2 SI for swallowing muscle volumes-of-interest (VOIs) were collected and delta SI changes (Δ) were calculated. Mid- and post-RT SI relative to baseline were assessed and correlations between radiation dose and percent change in SI were calculated. Independent samples t-tests were used to compare the percent change of SI between patients divided into two groups based on dysphagia status post-RT.

Results: Forty-six patients with stage III/IV HPV+ OPC were included in this study. Relative to baseline, mean T2 and T1+C SIs for middle pharyngeal constrictor were both significantly higher at mid- and post-RT ($p<0.004$ for all). Superior pharyngeal constrictor also showed a significant increase in T1+C SI at mid-RT ($p=0.0004$). Additional muscle VOIs showed significant changes post-RT, but not earlier at mid-RT. Both mid- and post-RT dose were significantly correlated with the percent change of normalized T2 and T1+C SI for examined muscle VOIs ($p<0.002$). Mean percent changes of normalized T2 SI at mid-RT relative to baseline for all muscle VOIs were significantly higher in patients who developed grade ≥2 dysphagia relative to patients with no/mild dysphasia (mean Δ%: 8.2% vs 1.9%; respectively, $p=0.002$). However, at post-RT, these changes were only significant in T1 SI (11.2% vs −1.3%; $p<0.0001$).

Conclusion: Signal intensity kinetics of radiation injury can be broadly correlated with functional muscular defect. Serial MRI during the course of RT may provide an opportunity to quantitatively track muscular pathology for subclinical detection of patients at high risk to develop dysphagia.

Keywords

Head and neck cancer; radiation-associated dysphagia; MRI; imaging biomarkers; HPV-associated oropharyngeal cancer

Introduction

In the modern era, favorable oncologic and survival outcomes are achieved for many patients with head and neck squamous cell carcinoma (HNSCC) treated with curative-intent radiotherapy (RT)[1–3], particularly for those with human papilloma virus (HPV) associated disease[4, 5]. Consequently, there is now substantial emphasis on reduction of late radiation toxicities for the ever increasing numbers of long-term survivors[5]. As burden of xerostomia is partially mitigated by the use of more conformal treatment techniques such as intensity modulated radiotherapy (IMRT) and proton therapy[6–8], dysphagia has overtaken as a primary driver of quality of life in HNSCC survivorship[9]. Up to 30% of survivors develop chronic aspiration even with modern RT techniques [10, 11] and this is typically not diagnostically appreciated until months or years after the completion of RT when symptoms manifest, making early identification and prediction of treatment-related dysphagia a major unmet need[12].

In recent years, the role of imaging in radiation oncology evolved beyond clinical staging and anatomical precision for RT planning as imaging parameters began to be integrated in dose-response models for the prediction of toxicity outcomes.[13–16] Owing to versatility to

provide soft tissue detail together with quantitative functional data, magnetic resonance imaging (MRI) is used to investigate changes induced by RT in the non-target normal tissue of the head and neck[16, 17]. Our group previously published [15] the feasibility of MRI to detect RT dose-dependent changes in signal intensity (SI) of pharyngeal wall muscles in a retrospective series of nasopharyngeal cancer patients treated with definitive RT, but the functional relevance of this SI parameter was not clear as the retrospective dataset did not have available relevant functional outcomes data. Thus, prospective data in a homogenous dataset of HNSCC patients with a standardized MRI acquisition parameters is required to validate and expand our previous findings. To this end, we sought to explore whether SI kinetics obtained from serial MRI in non-target swallowing muscles could serve as a potential imaging biomarker of radiation-associated dysphagia through the following objectives to 1) characterize MRI signal intensity (SI) kinetics in the acute RT period in a prospective dataset of HPV+ OPC patients receiving curative intent RT, 2) determine the feasibility of using MRI as a tool to monitor dose dependent radiation-induced changes in the muscles of deglutition, and 3) correlate alteration in muscle specific SI changes from baseline over the course of therapy (mid- and post-RT) with dysphagia status as assessed by a validated videofluoroscopy-derived pharyngeal dysphagia grading system[18].

Methods and Materials

Patients

The parent randomized clinical trial (2012–0825) and correlative analyses (RCR03–0800 and PA11–0809) were approved by the Institutional Review Board of the University of Texas, MD Anderson Cancer Center. The Data Safety Monitoring Board approved the release of the data for this analysis. Data were collected from the electronic medical records for the enrolled patients with OPC who had been treated with curative intensity modulated RT (IMRT) or intensity modulated proton therapy (IMPT) concurrent with chemotherapy between February 2013 and November 2015 as part of an ongoing randomized clinical trial [19]. Trial participants who met the following criteria were eligible to participate in optional imaging studies: 1) pathologically proven OPC SCC, 2) above 18 years of age 3) P16 positivity by immunohistochemical assessment, 4) no prior head and neck RT, 5) ECOG performance status of 0–2, 6) no claustrophobia nor contraindications to MRI contrast agent, and 7) no previous primary cancer except well treated localized epithelial skin cancer.

MRI protocol

MRI examinations were performed on a 3.0-T GE Discovery 750 MRI scanner (GE Healthcare, Waukesha, WI, USA) with customized immobilization devices (Klarity Medical Products, Newark, OH, USA) in the same position used for the daily delivery of RT at three different time points; before the beginning of treatment as well as mid- (3–4 weeks after first RT fraction) and post-treatment (6–8 weeks after last RT fraction). Patient images at mid- and post-RT were indexed to those obtained pretreatment using the same immobilization devices utilized for daily image-guided therapy as detailed in Ding et al [20]. Geometrical scan parameters were prescribed for a standardized spatial region encompassing the palatine process region cranially to the cricoid cartilage caudally. Field of view (FOV) was 256 mm, number of slice= 30, spatial resolution= $1\times1\times2.5$ mm^3, and space between slices was 4 mm.

T2 weighted (T2w) and T1 weighted (T1w) pre- and post-contrast (Gadopentetate dimeglumine, Bayer Healthcare Pharmaceuticals) images were acquired using a fast spin-echo sequence (T2w: TR/TE= 3.7 s/103 ms, echo train length (ETL) = 16, NEX= 2, pixel bandwidth = 195 Hz; T1w: TR/TE= 630/7 ms; ETL = 2, NEX = 2, pixel bandwidth= 195 Hz; post-contrast T1w with fat saturation: TR/TE= 705/10 ms, ETL= 2, NEX= 2, pixel bandwidth= 98 Hz).

Radiation therapy

All patients underwent non contrast-enhanced computed tomography simulation in the immobilization devices as described previously.[21] At least 2 experienced radiation oncologists examined all patients and reviewed all the contours for quality assurance [21, 22]. In patients receiving IMRT, the Gross tumor volume plus margins received 70 Gy in 33 fractions. A relative biological effectiveness value of 1.1 was prescribed for IMPT patients. IMPT cases were planned with an Eclipse proton therapy treatment planning system (version 8.9, Varian Medical Systems, Palo Alto, California). IMRT planning was performed with a Pinnacle planning system (Philips Medical Systems, Andover, MA).

Chemotherapy

Patients received induction and/or concurrent chemotherapy as part of a standard of care regimen as detailed in Table 1.

Image segmentation and registration

For 10 patients, we performed manual segmentation using pre-treatment T1 sequences for the following non-target swallowing muscles at risk; superior pharyngeal constrictor (SPC), middle pharyngeal constrictor (MPC), intrinsic tongue (IT), geniohyoid (GH), genioglossus (GG), mylohyoid (MH), masseters (MM), medial pterygoids (MP), lateral pterygoids (LP), anterior digastric (AD), posterior digastric (PD), and buccinators (BUC) muscles. Auto-segmentation atlas was then developed using the manually segmented volumes of interest (VOIs) library in a commercial auto-segmentation software; (ADMIRE version 1.13.5, 2016). The muscle VOIs library was then used to auto-segment the remaining patient's pretreatment T1 images.

Deformable image registration (DIR) was performed between the different MRI time points using the benchmarked commercially available image registration software (Velocity AI, version 3.0.1, Atlanta, GA). All the VOIs were then propagated from pre-treatment T1 sequences to the different MRI sequences (i.e. T1+C and T2w) as well as the two other time points (mid- and post-RT). This was followed by QA review and manual editing whenever needed of all the contours by three expert radiation oncologists (CDF, ASRM, MAMM). Figure 1 shows an example of VOIs muscle library.

The MRI mean signal intensities (SIs) of the VOIs were collected and normalized, in the manner of Popovtzer et al [23], to an area in the cerebellum receiving negligible dose of RT (i.e. <15 Gy cumulative dose) to account for MRI variability at different time points. This was achievable for all patient except for three subjects who had 15–20 Gy in the reference normalization region. Percent change of each VOI SI from baseline was calculated using the

following formula [((mid or post-RT normalized SI – pre RT normalized SI) ÷ (pre RT normalized SI)) ×100]. The IMRT and IMPT plans were restored. Serial T1, T1+C and T2-weighted MRIs were co-registered with the treatment planning computed tomography images and the radiation dose grid to determine the dose-SI kinetics relationship for all VOIs.

Dysphagia classification

Dysphagia severity was graded according to the published Dynamic Imaging Grade for Swallowing Toxicity (DIGEST) criteria [18]. DIGEST is a validated, MBS-based severity staging tool for pharyngeal phase dysphagia. The summary DIGEST grade is based on the interaction of two domains: 1) swallow safety and 2) efficiency. To derive the safety profile, the rater assigns the maximum Penetration-Aspiration Scale (PAS) [24] observed across a series of standard bolus trials with a modifier applied to account for the frequency and amount of penetration/aspiration events. To derive the efficiency profile, the rater assigns an estimation of the maximum percentage of pharyngeal residue on an ordinal scale (<10%, 10–49%, 50–90%, and >90%) with modifiers to assign a pattern of residue across bolus types. The summary DIGEST rating aligns with NCI's Common Terminology Criteria for Adverse Events framework[25] for toxicity reporting in oncology trials and assigns a global rating of pharyngeal swallow safety and efficiency according to the interaction of the safety and efficiency profile scores (grade 0=no pharyngeal dysphagia, 1=mild, 2=moderate, 3=severe, 4=life threatening).

Statistical analysis

The time-interval-dependent T1, T1+C and T2-muscle signal alterations were measured **to characterize MRI signal intensity (SI) kinetics in muscles of swallowing.** Normalized SI changes were computed over the three time points, and changes relative to baseline were assessed using a paired t-test with a Bonferroni-corrected significance level of 0.004 (0.05/12) as a pre-specification for multiple comparisons across 12 different muscle VOIs. Of specific interest for hypothesis generation were changes in T1, T1+C, and T2 SI alteration from baseline to the two follow-up imaging time points (i.e. mid- and post-RT), normalized to pre-therapy baseline images. Because of the variable RT dose received by different muscle VOIs, we first measured longitudinal changes within each muscle group separately to characterize the patterns of SI changes specific to the muscle of interest. Subsequently, an aggregate all muscles VOI sum of SI changes in all non-target swallowing muscles grouped together was also calculated.

Correlations were computed to examine the strength of the linear association between RT dose received by the muscle VOIs grouped together and the percent change of SI at the two different time points (relative to baseline). The strength of correlation can be assessed by the general guidelines; 0.1–0.3 small/weak correlation, 0.3–0.5 medium/moderate correlation and 0.5–1 large/strong correlation[26]. For this assessment, we used grouped rather than separate muscle VOIs to represent the whole range of dose-muscle SI changes relationship, as dose variability within individual muscles was lower.

To explore the association between DIGEST groups and the percent change of SI relative to baseline at mid- and post-RT, independent sample t-test was used to compare the percent change of SI in patient group who developed videofluoroscopy DIGEST score≥ 2 moderate/severe dysphagia versus 0–1 no/mild dysphagia at median 8-month post-RT. All statistical analyses were performed using JMP 11.2 Pro (SAS Institute, Cary, NC).

Results

Patients

Forty six patients were included in the study, all with AJCC stage III/IV HPV+ OPC. The demographic, disease, and treatment criteria are outlined in Table 1. Patients' median age at time of RT was 59 years (range 39–78), and the majority were male (42 patients, 91%). Almost all patients received concurrent chemotherapy (98%). The gross tumor volume received 70 Gy over 33 fractions, with 24 patients (52%) treated by IMRT and 22 (48%) treated by IMPT concurrent with chemotherapy. All patients performed pre-RT MRI in the same position using the same fixation method of the treatment session. Three (7%) patients missed the mid-RT MRI and 9 (20%) did not return back for the post RT MRI. Each patient completed MRIs at two different time points. All of the patients performed swallowing studies before the start of treatment, and 41 (89%) patients returned for swallowing studies. The median follow-up time was 7.8 months (range: 4–10 months) after RT, with 6-months being the desired follow-up target.

Longitudinal swallowing muscle MRI signal intensity kinetics

Figure 2 shows the difference in normalized SI changes across the three time points of MPC as well as all muscle VOIs in T1+C and T2 MRI parameters. Using paired t-tests, significant increases in the mean normalized T1+C and T2 signal intensity were noted in MPC at mid-RT relative to baseline (0.9×10^{3} vs 1.2×10^{3} and 0.6×10^{3} vs. 0.8×10^{3}), respectively ($p < 0.0006$ for both). SPC also showed a significant increase in T1+C signal intensity at mid-RT ($p=0.0004$). Furthermore, at post-RT, there was a significant increase from baseline in the normalized mean T1+C signal intensity with respect to the majority of VOIs: MPC, SPC, MP, MM, MH, GG, ITM, ADC and PDM ($p<0.004$ for all), while a significant increase in T2 mean SI was identified only for MPC muscle ($p= 0.001$). The remaining muscles did not show any significant changes in SI over time. Furthermore, there were no significant changes in the mean normalized T1 SI identified in any of the VOIs. The comparison of all muscle VOIs grouped together showed a statistically significant increase in both T2 and T1+C at both time points (mid- and post-RT) ($p< 0.001$). However, there were no statistically significant changes in T1 SI in grouped VOIs at either time point ($p>0.05$ for both).

Relationship between RT dose and MRI signal intensity kinetics

The dose received at mid-RT was significantly correlated, although weak magnitude, with the percent change of normalized T1+C and T2 SI for the muscle VOIs ($r=0.14$, R-square 0.02, $p=0.002$ and $r=0.2$, R-square 0.04, $p<0.0001$) respectively. Similarly at post-RT, the dose was significantly correlated with the percent change of T1+C ($r=0.14$, R-square 0.02, $P= 0.0004$) and T2 SI ($r=0.24$, R-square 0.06; $p<0.0001$) as illustrated in Figure 3. However,

both mid- and post-RT doses were not correlated with T1 SI changes in the examined muscle VOIs.

Figure 4 illustrates two examples of MRI subtraction images intended to provide a visualization of the SI changes over time. The subtraction of the pre-RT images from the mid- and post-RT sequences demonstrates the visible (and quantifiable) increase in the SI of the MPC in T2 sequence and SPC in T1+C sequence.

Relationship between dysphagia (per DIGEST) and MRI signal intensity kinetics

At Pre-RT, all patients performed the swallowing studies contributing the following DIGEST distribution: 25 patients (54%) grade 0, 18 (39%) grade 1 “mild”, and 3 (7%) grade 2 “moderate”. None of the patients had tumor-associated severe dysphagia on baseline videofluoroscopy (DIGEST grade ≥ 3) pre-RT. Forty one patients returned for follow-up after RT and presented with the following DIGEST distribution: (17%) grade 0, 18 (44%) grade 1 “mild”, 11(27%) grade 2 “moderate”, and 5 (12%) grade 3 “severe” fluoroscopy detected dysphagia after RT at median 7.8 months (4–10 months). Two patients, with grade 2 before RT, remained as grade 2 after RT. These two patients were excluded from the analysis of the DIGEST due to the uncertainty of the attribution of moderate dysphagia post-RT to RT injury (versus tumor/comorbidity). The remaining 39 patients were classified into two groups: 1) patients converted to moderate or severe post-RT (new DIGEST grade ≥2 post-RT, n=14/39, 36%), and 2) no or mild post-RT dysphagia (DIGEST grade 0–1 post-RT, n=25/39, 64%). The percent change of normalized SI at mid-RT for all of the muscles grouped together was significantly higher in the group of patients who developed radiation induced moderate/severe dysphagia compared to the other patients, and this finding was observed in T2 (8.2% vs 1.9% $p=0.002$) but not in the other tested parameters. However at post-RT, these changes were only significant in T1 (11.2% vs −1.3% $p<0.0001$). Figure 5 shows the significant difference between the percent changes of SI at different time points and DIGEST score.

Discussion

Treatment-related sequelae such as mucositis and dysphagia have been claimed as the “barrier to win the battle” against HN cancer [27, 28]. The current study is a successful extension of our developing effort to integrate MRI biomarkers [18, 29–31] to characterize and reduce radiation induced normal tissue toxicities such as dysphagia. This continuous effort aims to adapt the RT dose and volume, particularly in patients with low-intermediate risk HPV+ OPC [32–35] and also to establish methods to identify high risk patients for earlier, intensive interventions before often irreversible symptoms manifest [18, 36, 37]. To the best of our knowledge, the present analysis is the first comparative study investigating the association between dysphagia severity according to DIGEST grade, dose to dysphagia-related structures, and MRI SI changes of deglutitive muscles in HPV+ OPC patients. Our results demonstrated proof of principle and feasibility of serial MRI acquisition to track SI kinetics of the pathological changes in non-target dysphagia-related muscles before, during and after RT, and suggest the potential for these parameters to serve as early imaging biomarkers of functionally relevant normal tissue injury before late effects manifest.

Previous work supports the premise that physiological mechanisms underlying soft tissue changes, such as edema, fibrosis, and fatty degeneration[38–40] can be quantified by MRI SI changes[41]. T2 signal alteration has long been associated with muscle injury in a variety of disease states[42], and has been held forth by Damon et al. as an established biomarker of muscle injury and inflammation; to wit, “Collectively, ... data strongly support the use of T2 as a biomarker for assaying longitudinal changes in muscle health”, as “T2 values are elevated in inflammation.”[43] Consequently, the finding of T2 SI alteration observed in our dataset is consistent broadly with inflammatory injury and acute edema of muscle secondary to radiotherapy [44]; however, to our knowledge, this is the first prospective characterization of the temporal course of this acute effect with spatial mapping to radiotherapy dose. Likewise, the kinetics of T2W alteration matched closely with the clinical timelines for acute radiotherapy-attributable inflammation to decline in follow-up, and thus are consistent with the self-limiting acute phase of radiation injury for normal tissue (e.g. acute radiotherapy-related mucositis or acute xerostomia).

Moreover, late post-therapy T1W intensity changes, which have been associated with late muscle injury generally, [23, 45] as well as in the head and neck muscles and swallowing specifically [46]. Furthermore, data have shown that masticator muscle T1W signal abnormality after radiotherapy can be used as a predictor of trismus post-radiotherapy. Consequently, our work affirms inflammation and fibrotic degeneration involving dysphagia-related muscles [47] can be linked to RT-induced MRI SI changes for better assessment of inter-fraction soft tissue changes that could conceivably be detected during or early after RT before clinically detectable pharyngeal dysfunction manifests [48].

Our data demonstrated that specific MRI sequences are a promising tool to quantify dose–response MRI parameter kinetics, which aligns with published data [23]. Our group and others previously focused on post-RT SI changes in a later post-RT time when injury may already have become clinically detectable without the MRI data [23, 49]. Specifically, Popovtzer et al. [23] demonstrated that higher doses to the pharyngeal constrictors were associated with increases in T2-weighted MRI SI in a cohort of twelve HNC patients imaged three months after RT. The late SI changes align with results of our current study in which we observed that higher dose to swallowing muscles was associated with higher percent of normalized T1+C and T2 SI changes in those VOI on mid-RT and early post-RT scans. Previous retrospective work in nasopharyngeal cancer by our group [15] demonstrated a significant decrease in the T1 SI for SPC on late post-RT scans only in patients who received a mean dose >62.25 Gy but non-significant changes of T1 SI at early post-RT follow up regardless of dose. This earlier work seemed to suggest a significant role for T1 SI modifications as a biomarker for intermediate to late phenomena (e.g. fibrotic degeneration, the degree of functional impairment) rather than for acute phase modifications whereas T2 SI changes seemed the more likely parameter to be related to edema from acute RT injury. This trend in earlier T2 SI differential was consistent both in our present and previous work [15]. To the best of our knowledge, our results are the first to show the possibility of tracking normal tissue damage as early as the midpoint of the RT course. These preliminary observations support our long-term research effort to establish adaptive strategies for early HPV+ OPC responders [35].

Other than demonstrating the ability to detect dose-dependent quantitative morphological and radiological changes, our findings suggest functional relevance of tracking MRI SI changes in the deglutition muscles. Grouped as a whole VOI, degree of SI changes was significantly higher in patients who developed videofluoroscopy detected moderate-severe dysphagia per DIGEST (grade ≥2), which is a validated in-house assessment tool aligned to CTCAE framework for MBS-graded swallowing dysfunction. Whole VOI mid-treatment SI changes proved to be associated with moderate to severe dysphagia in T2 as early as mid-RT but not the other tested sequences (T1 or T1-C). Consistent with the above-discussed findings [15], whole VOI SI kinetics on post-RT scans (6 weeks) significantly associated with later dysphagia status (median 7.8 months) only for the T1 parameter (not T2 or T1-C). This suggests that, seeking the earliest detectable imaging biomarker, mid-RT T2 SI kinetic might be the best, earliest candidate parameter to predict risk of late radiation-induced dysphagia. Longitudinal differences further highlight the importance of studying serial MRI scans during RT, and for extended periods of follow up after RT, to better understand the trajectories of the SI kinetics and when parameters have most relevance.

Our data suggest that the kinetics of RT injury can be quantified using serial MRI and broadly correlated with functional muscular injury as early as the midpoint of RT delivery. One of the study limitations is the short duration of follow-up at this point of the study and we are planning to acquire more long-term follow-up MRIs as part of a recently activated clinical study at our institution (NCT03145077). An additional limitation is the fact that 9 patients have missed the post-RT MRI thereby had only two time points of assessment. Likewise, the overall sample size is relatively small (46 patients) and needs future expansion for validation purposes. Despite the statistically significant correlation between dose and MRI SI changes, the correlation remains weak with wide spread of the data points as in Figures 3 and 5, indicating that other factors beside the dose may be implicated in these muscle changes and ultimately dysphagia. We and others have previously identified some of these factors (e.g. age, clinical stage, disease subsite, and weight loss) that, in addition to dose parameters, were independently associated with the development of late dysphagia.[32, 50] Therefore, future efforts are needed to enroll more patients in these imaging studies to be able to build a robust multivariate model that considers the effect of all these variables.

Another limitation is that the relative biological effectiveness (RBE) may be variable for the proton treated patients and may suggest further changes in SI. Furthermore, the exact timing of imaging acquisition that represents the most indicative SI changes associated with dysphagia remains to be determined. Our institution has recently activated an imaging study (NCT03224000) with weekly MRI acquisition to further interrogate the timing that has the most predictive value for such toxicity. Nonetheless, these preliminary results support further investigations to define clinically meaningful utilization of serial imaging with MRI during the course of curative-intent RT for HNSCC for toxicity reduction efforts. Further confirmatory studies are warranted to test the applicability of our approach in the management of RT-induced toxicities. Ideally, this may contribute to identify subgroups of high risk patients who may be candidate to more aggressive supportive care paths and/or earlier, intensified swallowing therapy programs, although for the latter consensus is still lacking [51]. Moreover, the capability of predicting toxicity from in-treatment, dose-related MRI SI modifications may open doors to a clinically-driven adaptive RT for non-target

swallowing muscle preservation and improvement of the therapeutic ratio for RT in the setting of HPV+ OPC.

Supplementary Material

Refer to Web version on PubMed Central for supplementary material.

Acknowledgments

Funding sources and financial disclosures: This work is directly supported by the Andrew Sabin Family Foundation; Dr. Fuller is a Sabin Family Foundation Fellow. Drs. Mohamed, Lai, Hutcheson, and Fuller receive(d) funding support from the National Institutes of Health (NIH)/National Institute for Dental and Craniofacial Research (1R01DE025248–01/R56DE025248–01) and NIH/NCI Early Phase Clinical Trials in Imaging and Image-Guided Interventions Program (1R01CA218148–01). Dr. Fuller received/receives ferderal grant and/or salary support from: the NIH/National Cancer Institute (NCI) Head and Neck Specialized Programs of Research Excellence (SPORE) Developmental Research Program Award (P50CA097007–10) and Pau l Calabresi Clinical Oncology Program Award (K12 CA088084–06); a National Science Foundation (NSF), Division of Mathematical Sciences, Joint NIH/NSF Initiative on Quantitative Approaches to Biomedical Big Data (QuBBD) Grant (NSF 1557679); the NIH Big Data to Knowledge (BD2K) Program of the National Cancer Institute (NCI) Early Stage Development of Technologies in Biomedical Computing, Informatics, and Big Data Science Award (1R01CA214825–01); and the Cancer center Support Grant Radiation Oncology/Cancer Imaging Program Seed Grant (5P30CA016672). Dr. Fuller receives(d) industry grant support and speaker travel funding from Elekta AB. Dr. Meheissen received grant and/or salary support from the Ministry of Higher Education of Egypt. Dr. Frank is the Principle Investigator of the Head and Neck Phase II/III Randomized Trial of IMPT vs IMRT for Patients with Advanced Stage Oropharyngeal Tumors and receives financial support from the following NCI/NIH grants; 5P01CA02123934, 2U19CA021239–35, U10CA1095344, 1R03CA188162–01A1. Dr. Frank receives generous industry grant support for the phase III randomized trial from Hitachi Medical. Dr. Frank received funding support from the University of Texas MD Anderson Cancer Center (UTMDACC) Institutional Research Grant Program, the UTMDACC Sister Institution Network Fund, the UTMDACC Center for Radiation Oncology Research, the UTMDACC HI-CRSP Program, and from the Cancer Prevention & Research Institute of Texas (CPRIT). Dr. Frank has received funding support from ELEKTA AB. Dr. Frank is a paid consultant for Varian and is on Varian's particle therapy advisory board and translational science board.

References

[1]. Beadle BM, Liao KP, Elting LS, Buchholz TA, Ang KK, Garden AS, et al. Improved survival using intensity-modulated radiation therapy in head and neck cancers: a SEER-Medicare analysis. Cancer. 2014;120:702–10. [PubMed: 24421077]

[2]. Garden AS, Kies MS, Morrison WH, Weber RS, Frank SJ, Glisson BS, et al. Outcomes and patterns of care of patients with locally advanced oropharyngeal carcinoma treated in the early 21(st) century. Radiat Oncol. 2013;8:21. [PubMed: 23360540]

[3]. Yildirim G, Morrison WH, Rosenthal DI, Sturgis EM, Papadimitrakopoulou VA, Schwartz DL, et al. Outcomes of patients with tonsillar carcinoma treated with post-tonsillectomy radiation therapy. Head Neck. 2010;32:473–80. [PubMed: 19691110]

[4]. Human Papillomavirus and Oropharyngeal Cancer Survival. N Engl J Med. 2010;363:1576.

[5]. Fakhry C, Zhang Q, Nguyen-Tan PF, Rosenthal D, El-Naggar A, Garden AS, et al. Human Papillomavirus and Overall Survival After Progression of Oropharyngeal Squamous Cell Carcinoma. J Clin Oncol. 2014;32:3365–73. [PubMed: 24958820]

[6]. Bhide SA, Miah AB, Harrington KJ, Newbold KL, Nutting CM. Radiation-induced xerostomia: pathophysiology, prevention and treatment. Clin Oncol (R Coll Radiol). 2009;21:737–44. [PubMed: 19833490]

[7]. Hunter KU, Lee OE, Lyden TH, Haxer MJ, Feng FY, Schipper M, et al. Aspiration pneumonia after chemo–intensity-modulated radiation therapy of oropharyngeal carcinoma and its clinical and dysphagia-related predictors. Head Neck. 2014;36:120–5. [PubMed: 23729173]

[8]. Little M, Schipper M, Feng FY, Vineberg K, Cornwall C, Murdoch-Kinch C-A, et al. Reducing Xerostomia After Chemo-IMRT for Head and Neck Cancer: Beyond Sparing the Parotid Glands. Int J Radiat Oncol Biol Phys. 2012;83:1007–14. [PubMed: 22056067]

[9]. Wilson JA, Carding PN, Patterson JM. Dysphagia after nonsurgical head and neck cancer treatment: patients' perspectives. Otolaryngol Head Neck Surg. 2011;145:767–71. [PubMed: 21746839]

[10]. Bhayani MK, Hutcheson KA, Barringer DA, Lisec A, Alvarez CP, Roberts DB, et al. Gastrostomy tube placement in patients with oropharyngeal carcinoma treated with radiotherapy or chemoradiotherapy: Factors affecting placement and dependence. Head Neck. 2013;35:1634–40. [PubMed: 23322563]

[11]. Eisbruch A, Kim HM, Feng FY, Lyden TH, Haxer MJ, Feng M, et al. Chemo-IMRT of oropharyngeal cancer aiming to reduce dysphagia: Swallowing organs late complication probabilities and dosimetric correlates. Int J Radiat Oncol Biol Phys. 2011;81:e93–e9. [PubMed: 21592678]

[12]. Hutcheson KA, Lewin JS, Barringer DA, Lisec A, Gunn B, Moore MWS, et al. Late Dysphagia after Radiotherapy-Based Treatment of Head and Neck Cancer. Cancer. 2012;118:5793–9. [PubMed: 23640737]

[13]. Gaddikeri S, Gaddikeri RS, Tailor T, Anzai Y. Dynamic Contrast-Enhanced MR Imaging in Head and Neck Cancer: Techniques and Clinical Applications. American Journal of Neuroradiology. 2016;37:588–95. [PubMed: 26427839]

[14]. Dai YL, King AD. State of the art MRI in head and neck cancer. Clin Radiol. 2017.

[15]. Messer JA, Mohamed AS, Hutcheson KA, Ding Y, Lewin JS, Wang J, et al. Magnetic resonance imaging of swallowing-related structures in nasopharyngeal carcinoma patients receiving IMRT: Longitudinal dose-response characterization of quantitative signal kinetics. Radiother Oncol. 2016;118:315–22. [PubMed: 26830697]

[16]. Dynamic contrast-enhanced MRI detects acute radiotherapy-induced alterations in mandibular microvasculature: prospective assessment of imaging biomarkers of normal tissue injury. 2016;6:29864.

[17]. Astreinidou E, Roesink JM, Raaijmakers CP, Bartels LW, Witkamp TD, Lagendijk JJ, et al. 3D MR sialography as a tool to investigate radiation-induced xerostomia: feasibility study. Int J Radiat Oncol Biol Phys. 2007;68:1310–9. [PubMed: 17482767]

[18]. Hutcheson KA, Barrow MP, Barringer DA, Knott JK, Lin HY, Weber RS, et al. Dynamic Imaging Grade of Swallowing Toxicity (DIGEST): Scale development and validation. Cancer. 2017;123:62–70. [PubMed: 27564246]

[19]. Steven J Frank M Randomized Trial of Intensity-Modulated Proton Beam Therapy (IMPT) Versus Intensity-Modulated Photon Therapy (IMRT) for the Treatment of Oropharyngeal Cancer of the Head and Neck. 2017.

[20]. Ding Y, Mohamed ASR, Yang J, Colen R, Frank SJ, Wang J, et al. Prospective Observer and Software-based Assessment of Magnetic Resonance Imaging Quality in Head and Neck Cancer: Should Standard Positioning and Immobilization Be Required for Radiotherapy Applications? Pract Radiat Oncol. 2015;5:e299–e308. [PubMed: 25544553]

[21]. Blanchard P, Garden AS, Gunn GB, Rosenthal DI, Morrison WH, Hernandez M, et al. Intensity-modulated proton beam therapy (IMPT) versus intensity-modulated photon therapy (IMRT) for patients with oropharynx cancer – A case matched analysis. Radiother Oncol. 2016;120:48–55. [PubMed: 27342249]

[22]. Rosenthal DI, Asper JA, Barker JL Jr., Garden AS, Chao KS, Morrison WH, et al. Importance of patient examination to clinical quality assurance in head and neck radiation oncology. Head Neck. 2006;28:967–73. [PubMed: 16823872]

[23]. Popovtzer A, Cao Y, Feng FY, Eisbruch A. Anatomical changes in the pharyngeal constrictors after chemo-irradiation of head and neck cancer and their dose-effect relationships: MRI-based study. Radiother Oncol. 2009;93:510–5. [PubMed: 19520446]

[24]. Rosenbek JC, Robbins JA, Roecker EB, Coyle JL, Wood JL. A penetration-aspiration scale. Dysphagia. 1996;11:93–8. [PubMed: 8721066]

[25]. Ang KK, Harris J, Wheeler R, Weber R, Rosenthal DI, Nguyen-Tân PF, et al. Human Papillomavirus and Survival of Patients with Oropharyngeal Cancer. The New England journal of medicine. 2010;363:24–35. [PubMed: 20530316]

[26]. Cohen J Statistical Power Analysis for the Behavioral Sciences (2nd Edition). united states of america: Lawrence Erlbaum; 1988.

[27]. Skladowski K, Maciejewski B, Golen M, Pilecki B, Przeorek W, Tarnawski R. Randomized clinical trial on 7-day-continuous accelerated irradiation (CAIR) of head and neck cancer - report on 3-year tumour control and normal tissue toxicity. Radiother Oncol. 2000;55:101–10. [PubMed: 10799721]

[28]. Vokes EE, Stenson K, Rosen FR, Kies MS, Rademaker AW, Witt ME, et al. Weekly carboplatin and paclitaxel followed by concomitant paclitaxel, fluorouracil, and hydroxyurea chemoradiotherapy: curative and organ-preserving therapy for advanced head and neck cancer. J Clin Oncol. 2003;21:320–6. [PubMed: 12525525]

[29]. Lambrecht M, Van Calster B, Vandecaveye V, De Keyzer F, Roebben I, Hermans R, et al. Integrating pretreatment diffusion weighted MRI into a multivariable prognostic model for head and neck squamous cell carcinoma. Radiother Oncol. 2014;110:429–34. [PubMed: 24630535]

[30]. Kim S, Loevner L, Quon H, Sherman E, Weinstein G, Kilger A, et al. Diffusion-weighted magnetic resonance imaging for predicting and detecting early response to chemoradiation therapy of squamous cell carcinomas of the head and neck. Clin Cancer Res. 2009;15:986–94. [PubMed: 19188170]

[31]. Owadally W, Hurt C, Timmins H, Parsons E, Townsend S, Patterson J, et al. PATHOS: a phase II/III trial of risk-stratified, reduced intensity adjuvant treatment in patients undergoing transoral surgery for Human papillomavirus (HPV) positive oropharyngeal cancer. BMC Cancer. 2015;15:602. [PubMed: 26311526]

[32]. Beyond mean pharyngeal constrictor dose for beam path toxicity in non-target swallowing muscles: Dose-volume correlates of chronic radiation-associated dysphagia (RAD) after oropharyngeal intensity modulated radiotherapy. Radiother Oncol. 2016;118:304–14. [PubMed: 26897515]

[33]. Schwartz DL, Hutcheson K, Barringer D, Tucker SL, Kies M, Holsinger FC, et al. Candidate Dosimetric Predictors of Long-Term Swallowing Dysfunction After Oropharyngeal Intensity-Modulated Radiotherapy. International Journal of Radiation Oncology*Biology*Physics. 2010;78:1356–65.

[34]. Blanchard P, Wong AJ, Gunn GB, Garden AS, Mohamed AS, Rosenthal DI, et al. Toward a model-based patient selection strategy for proton therapy: External validation of photon-derived normal tissue complication probability models in a head and neck proton therapy cohort. Radiother Oncol. 2016;121:381–6. [PubMed: 27641784]

[35]. Schwartz DL, Garden AS, Shah SJ, Chronowski G, Sejpal S, Rosenthal DI, et al. Adaptive radiotherapy for head and neck cancer--dosimetric results from a prospective clinical trial. Radiother Oncol. 2013;106:80–4. [PubMed: 23369744]

[36]. Rosenthal DI, Lewin JS, Eisbruch A. Prevention and Treatment of Dysphagia and Aspiration After Chemoradiation for Head and Neck Cancer. J Clin Oncol. 2006;24:2636–43. [PubMed: 16763277]

[37]. Chen AY, Frankowski R, Bishop-Leone J, Hebert T, Leyk S, Lewin J, et al. The development and validation of a dysphagia-specific quality-of-life questionnaire for patients with head and neck cancer: the M. D. Anderson dysphagia inventory. Arch Otolaryngol Head Neck Surg. 2001;127:870–6. [PubMed: 11448365]

[38]. Lamminen AE, Tanttu JI, Sepponen RE, Suramo IJ, Pihko H. Magnetic resonance of diseased skeletal muscle: combined T1 measurement and chemical shift imaging. Br J Radiol. 1990;63:591–6. [PubMed: 2400872]

[39]. Hsu HY, Chai CY, Lee MS. Radiation-induced muscle damage in rats after fractionated high-dose irradiation. Radiat Res. 1998;149:482–6. [PubMed: 9588359]

[40]. Gillette EL, Mahler PA, Powers BE, Gillette SM, Vujaskovic Z. Late radiation injury to muscle and peripheral nerves. Int J Radiat Oncol Biol Phys. 1995;31:1309–18. [PubMed: 7713790]

[41]. Mukherji SK, Mancuso AA, Kotzur IM, Mendenhall WM, Kubilis PS, Tart RP, et al. Radiologic appearance of the irradiated larynx. Part I. Expected changes. Radiology. 1994;193:141–8. [PubMed: 8090882]

[42]. Ababneh Z, Beloeil H, Berde CB, Gambarota G, Maier SE, Mulkern RV. Biexponential parameterization of diffusion and T2 relaxation decay curves in a rat muscle edema model: decay curve components and water compartments. Magn Reson Med. 2005;54:524–31. [PubMed: 16086363]

[43]. Damon BM, Li K, Bryant ND. Magnetic resonance imaging of skeletal muscle disease. Handb Clin Neurol. 2016;136:827–42. [PubMed: 27430444]

[44]. May DA, Disler DG, Jones EA, Balkissoon AA, Manaster BJ. Abnormal signal intensity in skeletal muscle at MR imaging: patterns, pearls, and pitfalls. Radiographics. 2000;20 Spec No:S295–315. [PubMed: 11046180]

[45]. Glazer HS, Lee JK, Levitt RG, Heiken JP, Ling D, Totty WG, et al. Radiation fibrosis: differentiation from recurrent tumor by MR imaging. Radiology. 1985;156:721–6. [PubMed: 4023233]

[46]. Becker M, Schroth G, Zbaren P, Delavelle J, Greiner R, Vock P, et al. Long-term changes induced by high-dose irradiation of the head and neck region: imaging findings. Radiographics. 1997;17:5–26. [PubMed: 9017796]

[47]. Eisbruch A, Schwartz M, Rasch C, Vineberg K, Damen E, Van As CJ, et al. Dysphagia and aspiration after chemoradiotherapy for head-and-neck cancer: which anatomic structures are affected and can they be spared by IMRT? Int J Radiat Oncol Biol Phys. 2004;60:1425–39. [PubMed: 15590174]

[48]. Ohshio I, Hatayama A, Kaneda K, Takahara M, Nagashima K. Correlation between histopathologic features and magnetic resonance images of spinal cord lesions. Spine (Phila Pa 1976). 1993;18:1140–9. [PubMed: 8362319]

[49]. Nomayr A, Lell M, Sweeney R, Bautz W, Lukas P. MRI appearance of radiation-induced changes of normal cervical tissues. Eur Radiol. 2001;11:1807–17. [PubMed: 11511906]

[50]. Wopken K, Bijl HP, van der Schaaf A, van der Laan HP, Chouvalova O, Steenbakkers RJ, et al. Development of a multivariable normal tissue complication probability (NTCP) model for tube feeding dependence after curative radiotherapy/chemo-radiotherapy in head and neck cancer. Radiother Oncol. 2014;113:95–101. [PubMed: 25443500]

[51]. Perry A, Lee SH, Cotton S, Kennedy C. Therapeutic exercises for affecting post-treatment swallowing in people treated for advanced-stage head and neck cancers. Cochrane Database Syst Rev. 2016:Cd011112. [PubMed: 27562477]

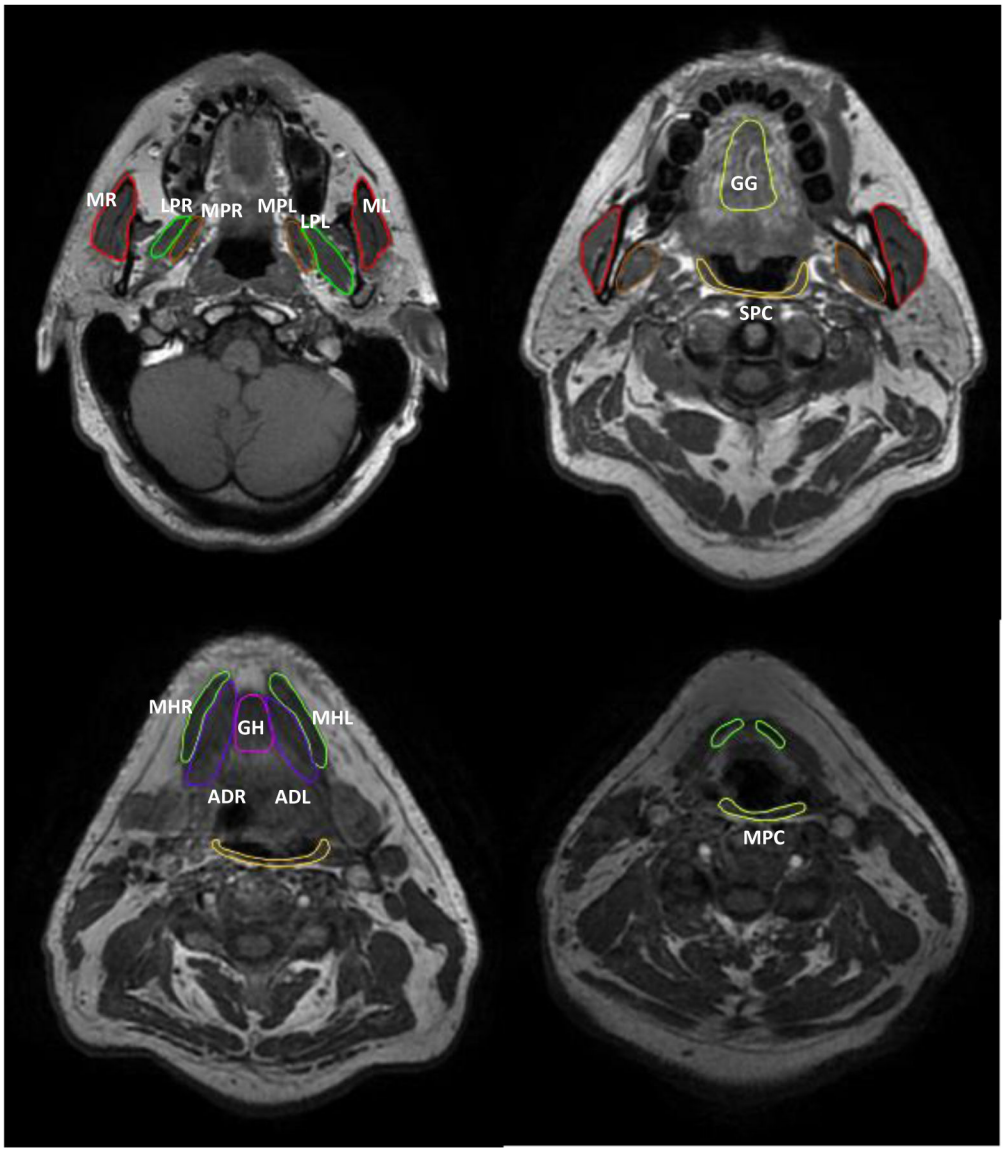

Figure 1.

Example of segmented muscle volumes of interest. *Abbreviations:* MR: right masseter, ML: left masseter, LPR: right lateral pterygoid, LPL: left lateral pterygoid, MPL: left medial pterygoid, MPR: right medial pterygoid, GG: genioglossus, GH: geniohyoid, MHL: left myelohyoid, MHR: right myelohyoid, ADR: right anterior digastric, ADL: left anterior digastric, SPC: superior pharyngeal constrictor, MPC: middle pharyngeal constrictor.

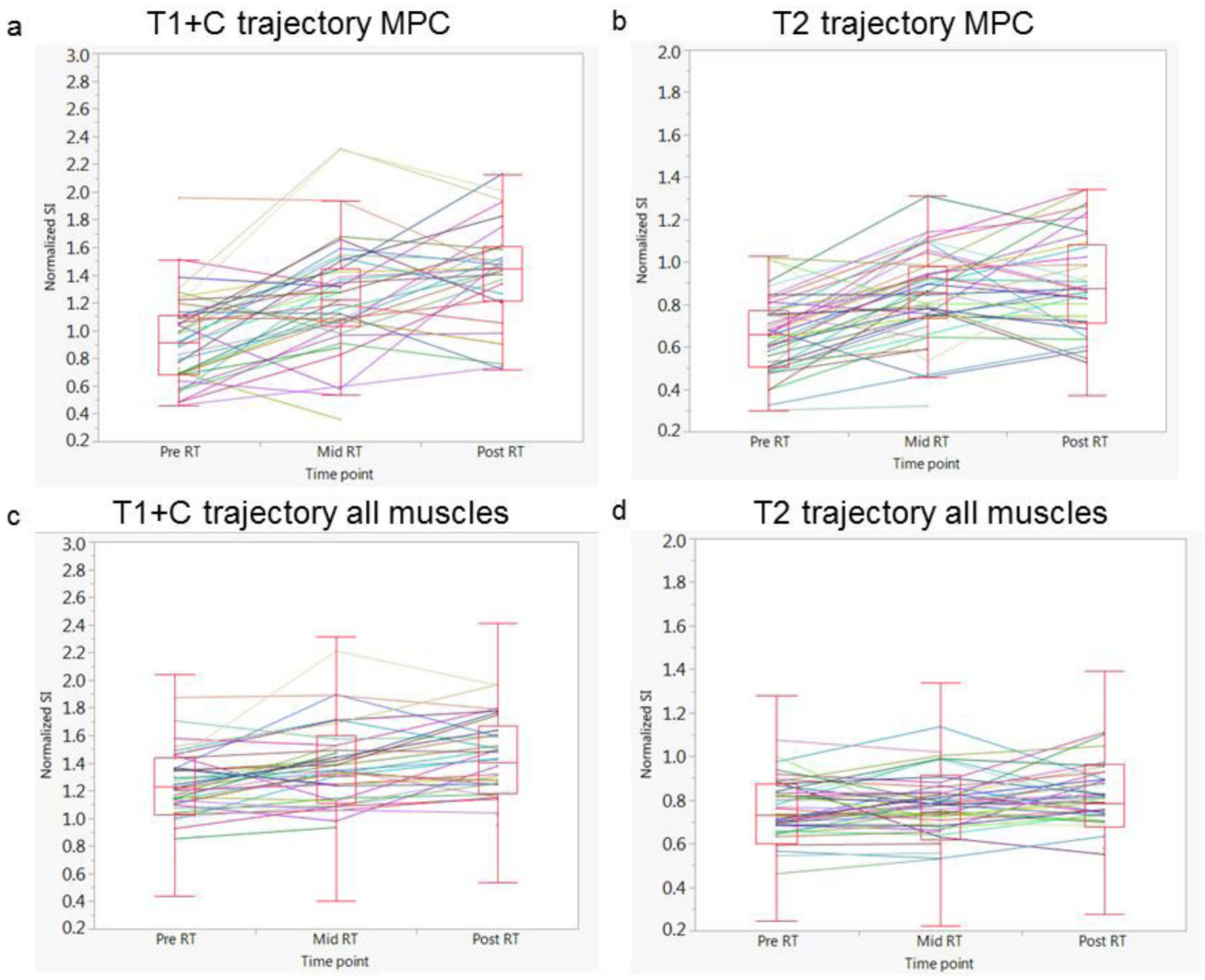

Figure 2.

Box plots depicting the distribution of normalized signal intensity over time. There is an overall significant increase in normalized SI over time of MPC muscle in T1+C (a) and T2 (b) sequences at both mid- and post-RT relative to baseline values ($p < 0.001$ for both), as well as in all the muscles grouped together in T1+C (c) and T2 (d) sequences ($p < 0.001$ for both). The solid lines depict the trajectory at the individual patient level.

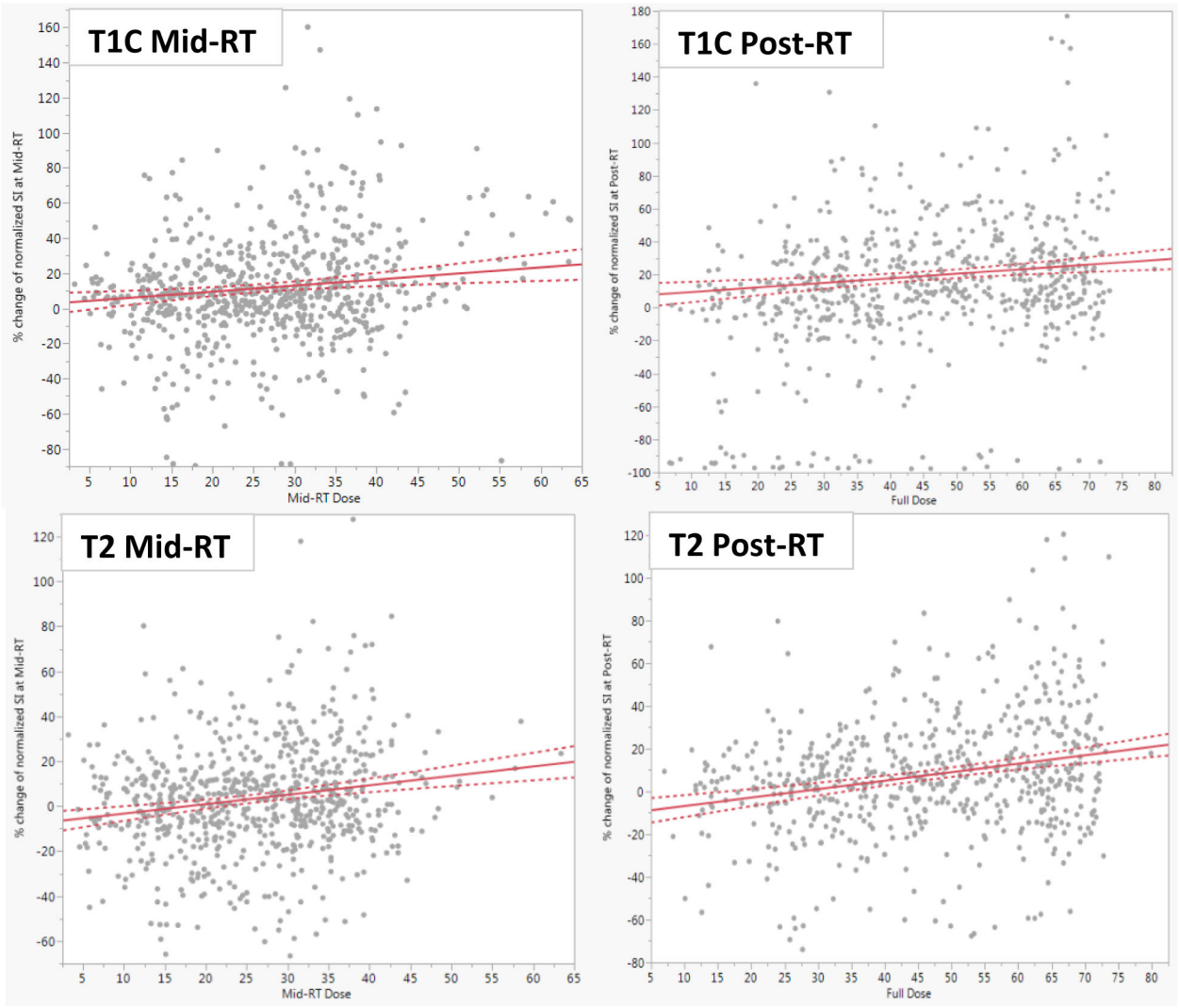

Figure 3.

Linear regression analyses identified positive correlations between the dose received at Mid- (left column) and Post-RT (right column) by the grouped muscle VOIs and the normalized SI of T1+C (upper row) and T2 (lower row) images. The dose received at mid-RT was significantly correlated, with the percent change of normalized T1+C and T2 SI for the muscle VOIs (r=0.14, R-square 0.02, p=0.002 and r=0.2, R-square 0.04, p<0.0001) respectively. Full dose was also significantly correlated with the percent change of T1+C (r=0.14, R-square 0.02, P= 0.0004) and T2 SI (r=0.24, R-square 0.06; p<0.0001)

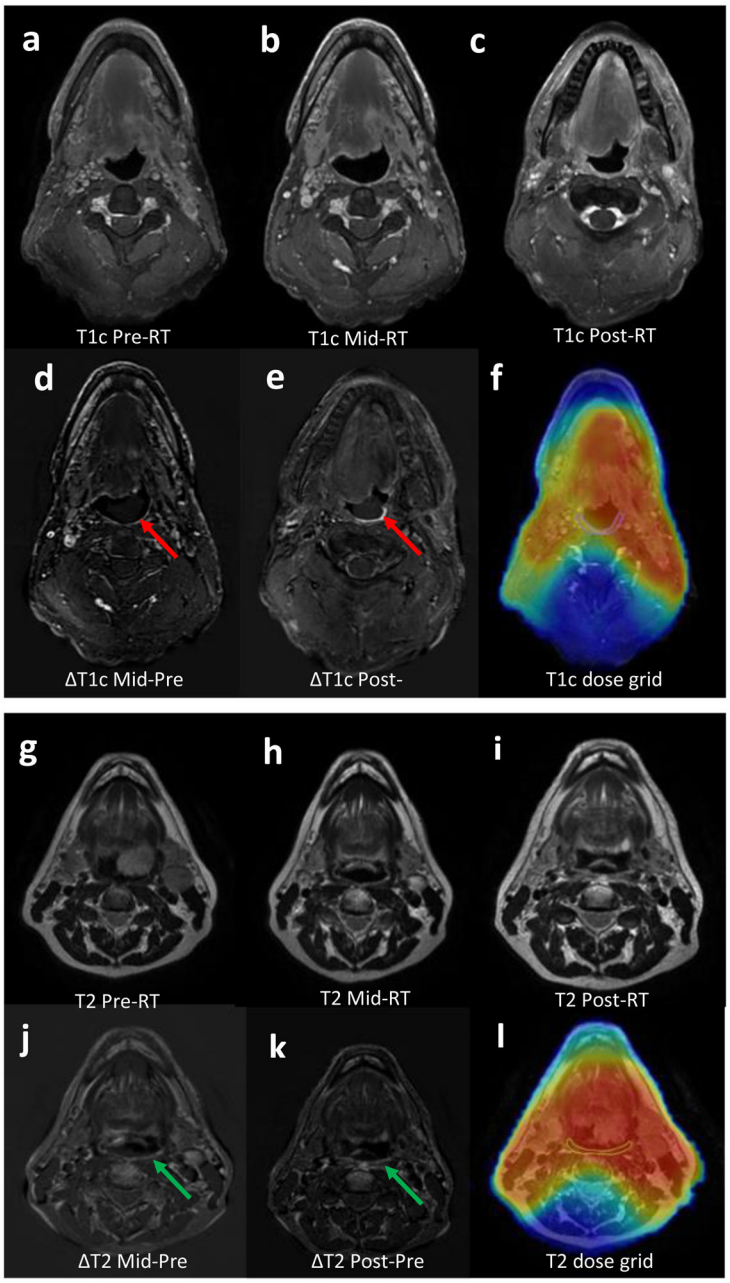

Figure 4.

Subtraction image of the pre-RT T1+C (4a) from mid-RT (4b) and post-RT (4c) showing the increase in SI of SPC demonstrating the edema that developed from RT at mid-RT(4d,red arrow) and more at post-RT (4e,red arrow) with the dose grid propagated from CT to T1+C sequence (4f). Another subtraction of the pre-RT T2 (4g) from both the mid-RT (4h) as well as the post-RT (4i) showing the RT-induced increase in SI of the MPC at mid-RT (4J,green arrow) and post-RT (4k,green arrow), with the dose grid over T2 showing the MPC located in the high dose region (4l)

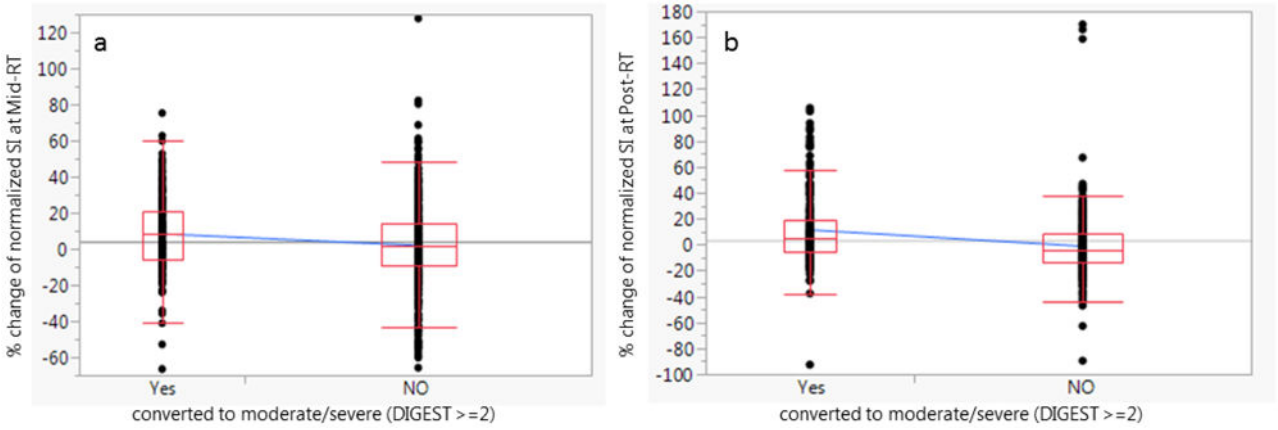

Figure 5.

The difference between the mean percent changes of SI at Mid-treatment T2 MRI parameter (8.2% vs 1.9%; p=0.002) (5a), and at post-treatment T1 (11.2% vs −1.3%; p<0.0001) (5b) between the two different groups of patients based on DIGEST score (converted post-RT grade≥2, moderate-severe dysphagia).

Table (1):

patient demographics (age, sex, and ethnicity). Tumor characteristics, radiotherapy and chemotherapy.

Characteristic	Result
Number of patients	46
Median age at time of RT	59 (39-78)
Sex, n (%)	
Male	42 (91%)
Female	4 (9%)
Ethnicity, n (%)	
Caucasian	41 (89%)
Black	3 (7%)
Hispanic	1 (2%)
Asian	1 (2%)
Tumor site, n (%)	
Base of tongue	26 (57%)
Tonsils	20 (43%)
TNM	
T1	3 (22%)
T2	17 (37%)
T3	10 (22%)
T4	16 (35%)
N1	5 (11%)
N2A	3 (7%)
N2B	17 (37%)
N2C	20 (43%)
N3	1 (2%)
Dose prescribed	70 Gy
Number of fractions	33
Type of RT n, (%)	
IMRT	24 (52%)
IMPT	22 (48%)
Induction Chemotherapy, n (%)	
Yes	10 (22%)
No	36 (78%)
Type of induction chemotherapy, n (%)	
PCC	3 (7%)
TPF	4 (9%)
Platinum/Taxanes	2 (4%)
Platinum single agent	1 (2%)
Concurrent chemotherapy, n (%)	
Yes	45 (98%)
No	1 (2%)

Characteristic	Result
Type of concurrent chemotherapy, n (%)	
Platinum single agent	39 (87%)
Taxanes	1 (2%)
Platinum/Taxanes	1 (2%)
Cetuximab	4 (9%)

TPF: docetaxel, cisplatin and fluorouracil

PCC: Paclitaxel, Carboplatin and Cetuximab